Ferrocene-Based Nanoelectronics: Regioselective Syntheses and Electrochemical Characterization of α-Monothiol and α,ω-Dithiol, Phenylethynyl-Conjugated, 2,5-Diethynylpyridyl- and Pyridinium-Linked Diferrocene Frameworks Having an End-to-End Distance of ∼4 nm

Chaiwat Engtrakul and Lawrence R. Sita*

Department of Chemistry and Biochemistry, University of Maryland, College Park, Maryland 20742

Received August 13, 2007

Regiospecific synthetic methods have been developed for the assembly of unsymmetric conjugated molecular frameworks containing 2,5-diethynylpyridyl- and 2,5-diethynylpyridinium-linked diferrocene structures and possessing either mono- or dithioacetate end-groups that are suitable for chemisorption onto Au(111) substrates after conversion to the corresponding thiol derivatives. Electronic spectra and solution electrochemistry of these and model compounds establish the electron-withdrawing character of a 2,5-dimethoxyphenylethynyl substituent on ferrocene that serves to shift the Fe(II)/Fe(III) redox couple to higher potentials. Further, while the unsymmetric nature of the 2,5-diethynylpyridyl bridge in **3** does not differentially perturb the redox couples of the two ferrocenes ($\Delta E_{1/2} < 10$ mV), upon methylation, the corresponding pyridinium moiety of **4** now produces a large separation in the two redox potentials ($\Delta E_{1/2} = 190$ mV). For the two regioisomeric monothioacetate compounds bearing a terminal 2,5-diethynylpyridyl-linked diferrocene unit, **5** and **6** (and their respective pyridinium counterparts, **7** and **8**), redox potentials of the two ferrocenes are found to be either widely separated or similar in value depending upon the added influence of the 2,5-dimethoxyphenylethynyl group (e.g., $\Delta E_{1/2} = 310$ mV in **7** vs ∼50 mV in **8**).

Introduction

Experimental and theoretical interest in the conduction physics of metal lead/molecule/metal lead (LML) heterojunctions remains unabated, and for good reason.[1] After electron transfer theory, which describes the coupling of electronic and nuclear motions as the basis for electronic transfer rates, a thorough understanding of the dependence of transport through LML heterojunctions as a function of molecular structure is the next logical step by which to further build the foundations of modern chemistry, as conductance directly measures the connection of wave functions between elements of a molecular framework and the response of these connections to an applied electron flux.[2] Further, just as the successful experimental validation of electron transfer theory found a wide range of applications, a unified molecular conductance theory will be critical to a large number of emerging, and as-of-yet-unforeseen, technologies, such as "molecular electronics", in which single molecules or molecular assemblies are envisioned as serving as components within nanoscale electronic devices.[1–3]

Unfortunately, after a decade of intense worldwide interest, investment, and investigation, both the development of a unified molecular conductance theory and the promise of molecular electronics have not yet materialized. In this regard, while significant experimental and theoretical advances have been made in the study of LML heterojunctions, the quantitative agreement between theory and experiment for the efficiency of electron transport in all-organic saturated or conjugated frameworks chemisorbed to gold electrodes through Au−S interactions, such as those containing *n*-alkyl, poly(phenyl), and poly(phenylethynyl) oligomers of general structure Au/−S−$(CH_2)_n$−S−/Au, Au/−S−$(C_6H_4)_n$−S−/Au, and Au/−S−$(C_6H_4$−C≡C$)_n$−C_6H_4S−/Au, respectively, is still off by orders of magnitude.[4,5] More specifically, experimentally measured current (*I*)−voltage (*V*) curves for all-organic LML heterojunctions uniformly exhibit a nonconducting region centered at zero bias that extends for several hundred mV and a first conductance maximum occurring at a relatively large bias of 1.5 V with a peak conductance in the nS range, which is about 500 times smaller than calculated. Several possible reasons for these discrepancies include remain-

* Corresponding author. E-mail: lsita@umd.edu.

(1) Heath, J. R.; Ratner, M. A. *Phys. Today* **2003**, *56*, 43–49.

(2) Nitzan, A.; Ratner, M. A. *Science* **2003**, *300*, 1384–1389.

(3) (a) Reed, M. A. *Nat. Mater.* **2004**, *3*, 286–287. (b) Wassel, R. A.; Gorman, C. B. *Angew. Chem., Int. Ed.* **2004**, *43*, 5120–5123.

(4) (a) Collier, C. P.; Wong, E. W.; Belohradsky, M.; Raymo, F. M.; Stoddart, J. F.; Kuekes, P. J.; Williams, R. S.; Heath, J. R. *Science* **1999**, *285*, 391–394. (b) Cui, X. D.; Primak, A.; Zarate, X.; Tomfohr, J.; Sankey, O. F.; Moore, A. L.; Moore, T. A.; Gust, D.; Harris, G.; Lindsay, S. M. *Science* **2001**, *294*, 571–574. (c) Holmlin, R. E.; Haag, R.; Chabinyc, M. L.; Ismagilov, R. F.; Cohen, A. E.; Terfort, A.; Rampi, M. A.; Whitesides, G. M. *J. Am. Chem. Soc.* **2001**, *123*, 5075–5085. (d) Salomon, A.; Cahen, D.; Lindsay, S.; Tomfohr, J.; Engelkes, V. B.; Frisbie, C. D. *Adv. Mater.* **2003**, *15*, 1881–1890. (e) Xu, B.; Tao, N. J. *Science* **2003**, *301*, 1221–1223. (f) Kushmerick, J. G.; Blum, A. S.; Long, D. P. *Anal. Chim. Acta* **2006**, *568*, 20–27. (g) Venkataraman, L.; Klare, J. E.; Tam, I. W.; Nuckolls, C.; Hybertsen, M. S.; Steigerwald, M. L. *Nano Lett.* **2006**, *6*, 458–462.

(5) (a) Seminario, J. M.; De La Cruz, C. E.; Derosa, P. A. *J. Am. Chem. Soc.* **2001**, *123*, 5616–5617. (b) Ke, S. H.; Baranger, H. U.; Yang, W. *J. Am. Chem. Soc.* **2004**, *126*, 15897–15904. (c) Xue, Y.; Ratner, M. A. *Phys. Rev. B: Condens. Mat. Mater. Phys* **2004**, *70*, 205416/1–205416/17. (d) Reimers, J. R.; Solomon, G. C.; Gagliardi, A.; Bilic, A.; Hush, N. S.; Frauenheim, T.; Di Carlo, A.; Pecchia, A. *J. Phys. Chem. A* **2007**, *111*, 5692–5702.

10.1021/om700807x CCC: $40.75
Publication on Web 02/08/2008

Scheme 1

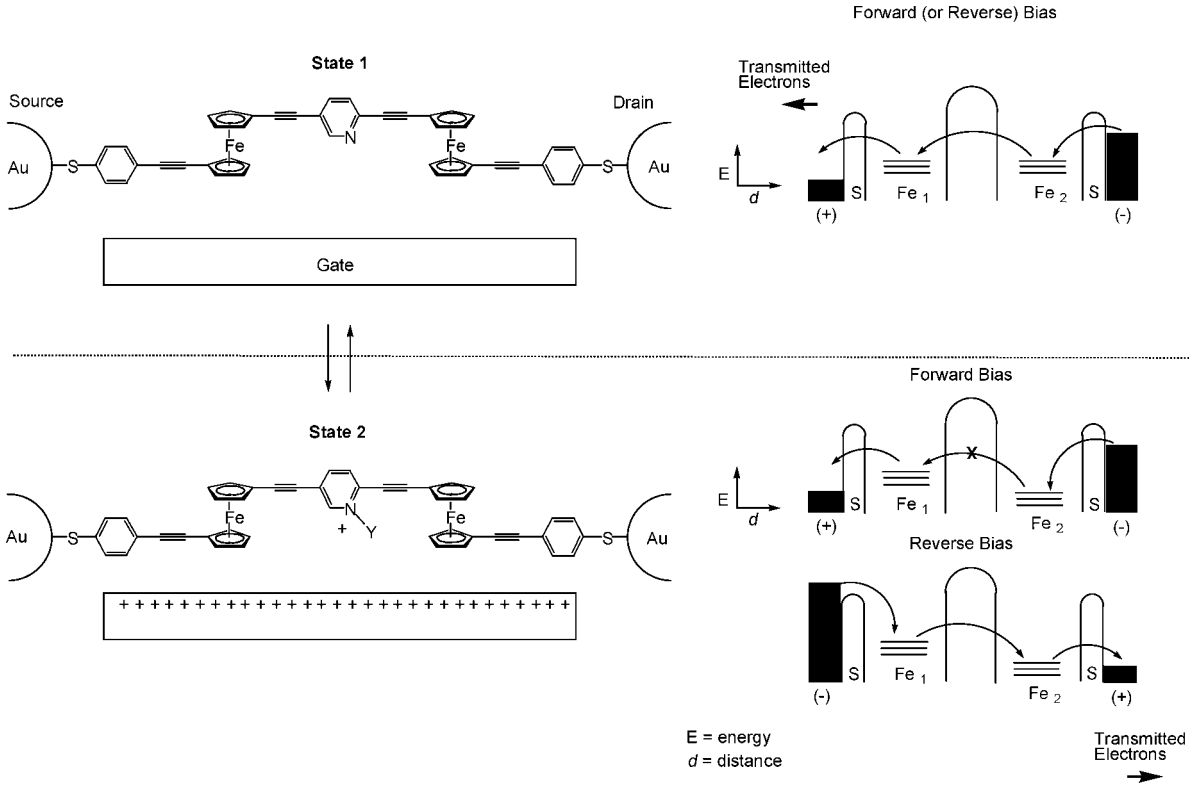

ing deficiencies and uncertainties with either the experimental designs employed to date, the nature of the molecular systems that have so far been chosen for study, or the present state-of-the-art of computational methods that have been developed to predict, in quantitative fashion, the conduction characteristics of such LML heterojunctions. Indeed, given the general fundamental electronic structure of organic frameworks, and even fully (highly) conjugated ones, all of these LML systems can be expected to possess electronic states for the organic bridge that are well above and below the effective Fermi level of the two metal leads, thereby, at a minimum, limiting transmission efficiencies and the ability to influence the energy levels of these electronic states relative to the effective Fermi level by application of a bias to a third gate electrode in more advanced LML configurations.

Given the possible intrinsic limitations of LML heterojunctions that are based on all-organic frameworks, we began an experimental program several years ago to explore the design, construction, and conduction physics of LML heterojunctions that incorporate transition metal-containing molecular frameworks due to the simple *a priori* expectation that they should possess low-lying metal-centered electronic states that can be more easily brought into resonance with the effective Fermi level of the leads.[6–8] In addition to potentially providing for higher transmissions at lower bias, intrinsically small energy differences between these electronic states, in conjunction with the spin properties of the transition metal ions, might also give rise to unique and signature spin crossover behavior that could then be probed and verified by bringing in additional parameters into play (e.g., variable-temperature and magnetic field studies).[8b,8b,9] Finally, resonant conduction through low-lying metal-centered states might well occur closer to equilibrium in these metal-containing LML heterojunctions, and thus, they may be more amenable to evaluation by present state-of-the-art computational methods.[10] In this respect, in 2001, we had introduced the design shown in Scheme 1 for a ferrocene-based molecular diode in which rectification of electron transport through a molecular framework might be mediated by an applied gate voltage.[6] Our initial communication also provided experimental support for the concept of utilizing the unsymmetric 2,5-diethynylpyridyl bridge between two ferrocene moieties for this purpose through the synthesis and electrochemical characterization of model complexes for States 1 and 2 in solution. Left unaddressed by these promising results, however, were two unknowns that could potentially prove to be significant obstacles to the eventual realization of Scheme 1. First is the synthetic challenge presented in making the required unsymmetric diferrocene frameworks that are long enough (e.g., ~3–4 nm) to reliably span the distance between two closely fabricated metal leads. Second, with this required molecular length, it is not immediately obvious that the diferrocene structures of Scheme 1 are capable of supporting efficient electron transport either via an "electron-hopping" mechanism involving distinct and spatially defined metal-centered molecular states or via a "through-bond" mechanism involving electron tunneling by way

(6) Engtrakul, C.; Sita, L. R. *Nano Lett.* **2001**, *1*, 541–549.

(7) Getty, S. A.; Engtrakul, C.; Wang, L.; Liu, R.; Ke, S.-H.; Baranger, H. U.; Yang, W.; Fuhrer, M. S; Sita, L. R. *Phys. Rev. B* **2005**, *71*, 241401/1–241401/4.

(8) For other experimental investigations of LML heterojunctions incorporating inorganic- or organometallic-based molecular frameworks, see: (a) Park, J.; Pasupathy, A. N.; Goldsmith, J. I.; Chang, C.; Yaish, Y.; Petta, J. R.; Rinkoski, M.; Sethna, J. P.; Abruna, H. D.; McEuen, P. L.; Ralph, D. C. *Nature* **2002**, *417*, 722–725. (b) Liang, W.; Shores, M. P.; Bockrath, M.; Long, J. R.; Park, H. *Nature* **2002**, *417*, 725–729. (c) Kim, B.; Beebe, J. M.; Olivier, C.; Rigaut, S.; Touchard, D.; Kushmerick, J. G.; Zhu, X. Y.; Frisbie, C. D. *J. Phys. Chem. C* **2007**, *111*, 7521–7526.

(9) Liu, R.; Ke, S.-H.; Baranger, H. U.; Yang, W. *Nano Lett.* **2005**, *5*, 1959–1962.

(10) Liu, R.; Ke, S.-H.; Baranger, H. U.; Yang, W. *J. Am. Chem. Soc.* **2006**, *128*, 6274–6275. Liu, R.; Ke, S.-H.; Yang, W.; Baranger, H. U. *J. Chem. Phys.* **2006**, *124*, 024718/1–024718/5.

Chart 1

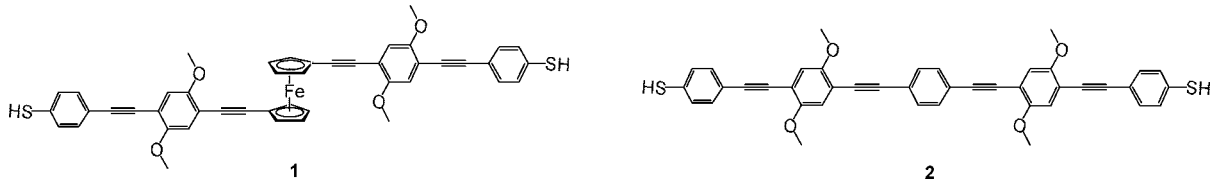

Chart 2

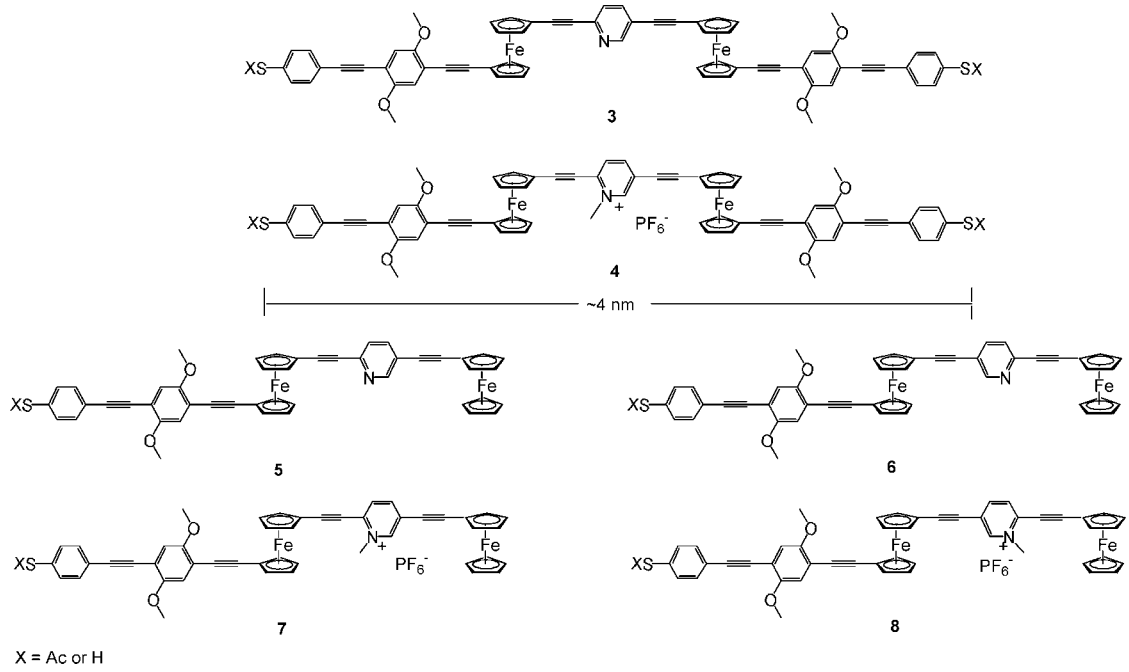

Scheme 2

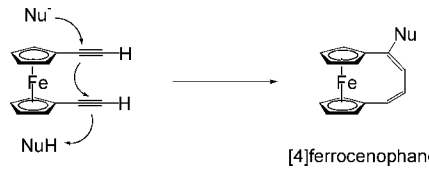

Scheme 3[a]

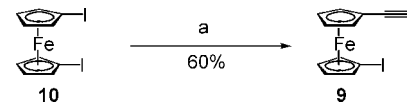

[a] (a) (i) HC≡CSi(^{i}Pr)$_3$, Pd(PPh$_3$)$_2$Cl$_2$, Cu(OAc)$_2$·H$_2$O, diisopropylamine (DIPA), 70° C, 24 h. (ii) TBAF (1.1 equiv), CH_2Cl_2, rt, 15 min.

of a single electronic state that is delocalized over the entire length of the system. Fortunately, in addressing the latter of these concerns first, we recently reported single-molecule measurements that show that conductance through LML heterojunctions derived from chemisorbtion of the monoferrocene dithiol **1** across the nanogap of electromigrated Au leads can exceed 70% of the theoretical limit at a bias of less than 100 mV.[7]

Importantly, while the overall bias-dependent conductance of LML heterojunctions derived from **1** is well explained by transport through a single molecular state that is strongly coupled to the macroscopic metal (Au) electrodes,[11] conductance through the corresponding ferrocene-absent LML heterojunction that is based on the all-organic phenylethynyl dithiol molecular framework of chemisorbed **2** shown in Chart 1 is at least 2 orders of magnitude lower and Coulomb-blockaded over several hundred mV.

Encouraged by the high transmission efficiency observed for LML heterojunctions based on **1**, the present report serves to bring the design shown in Scheme 1 a step further to final evaluation through the development of regiospecific synthetic routes to the unsymmetric thioacetate (thiol)-terminated diferrocene compounds **3**−**8** shown in Chart 2 that are suitable for chemisorption onto metal (Au) supports, which in the case of self-assembled monolayer (SAM) test structures based on the monothiols **6**−**8**, can be incorporated in regiospecific fashion with the nitrogen directed either toward or away from the Au surface with known certainty. Electronic spectra and solution electrochemistry of **3**–**8** and related model compounds further serve to establish the electron-withdrawing character of a 2,5-dimethoxyphenylethynyl substituent on ferrocene that manifests as a shift of the Fe(II)/Fe(III) redox couple to higher potentials.[12] Finally, for the sake of completeness and future reference, a detailed account of the synthesis of **1** is reported here for the first time as well.

(11) (a) Landauer, R. *IBM J. Res. Dev.* 1957, *1*, 233. (b) Datta, S. *Electronic Transport in Mesoscopic Systems*; Cambridge University Press: Cambridge, 1995.

(12) Results obtained regarding the fabrication and electrochemical characterization of SAMs derived from chemisorption of compounds **5** and **6**, as well as their pyridinium-protonated forms, will be presented elsewhere.

Scheme 4[a]

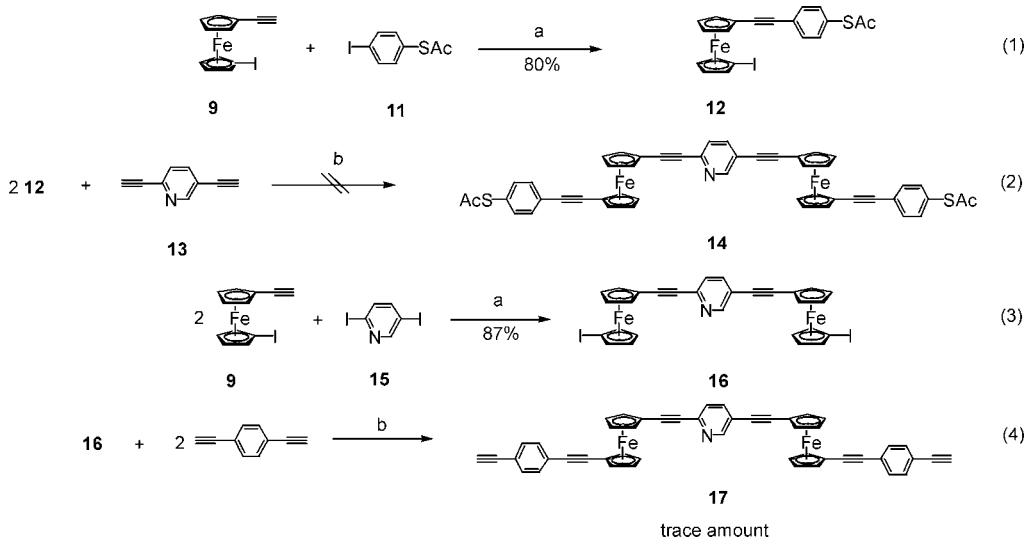

[a] (a) $Pd(PPh_3)_2Cl_2$, CuI, THF/diethylisopropylamine (Hunig's base) (1:1), 55° C, 24 h. (b) $Pd(PhCN)_2Cl_2$, CuI, P(*t*-Bu)$_3$, diisopropylamine (1.2 equiv), THF, 50° C, 24 h.

Scheme 5[a]

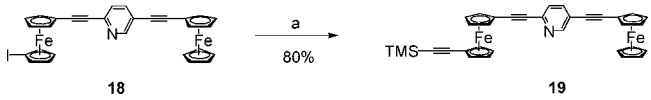

[a] (a) $HC{\equiv}CSi(Me)_3$, $Pd(PPh_3)_2Cl_2$, CuI, THF/Hunig's base (1:1), 50° C, 24 h.

Scheme 6[a]

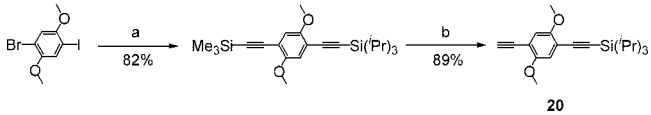

[a] (a) (i) $HC{\equiv}CSi(^iPr)_3$, $Pd(PPh_3)_2Cl_2$, CuI, DIPA, rt, 24 h. (ii) $HC{\equiv}CSiMe_3$, rt, 24 h. (b) 1 M NaOH, THF, MeOH, rt, 3 h.

Results and Discussion

(a) Synthesis of Diferrocene Frameworks. From the outset, it was quickly realized that construction of the desired target 2,5-diethynylpyridine-linked diferrocene adsorbates required to test the proposal of Scheme 1 would present some significant synthetic challenges. The heart of these problems centered on the need to identify a suitable ferrocene building block that could be used to construct extended conjugated molecular frameworks in an orthogonal (i.e., unsymmetric) fashion. Thus, while several different structural classes of ferrocene with two symmetrically disposed alkyne substituents in the 1,1′-positions have been previously reported,[13] to the best that we can ascertain, only one family of unsymmetrically substituted 1,1′-dialkyne ferrocene derivatives is known.[14] Further complicating potential synthetic routes to these compounds is the known ease with which 1,1′-diethynylferrocene apparently undergoes facile nucleophilic attack at the β-carbon of an ethynyl group and subsequent cyclization to produce a [4]ferrocenophane structure

Scheme 7[a]

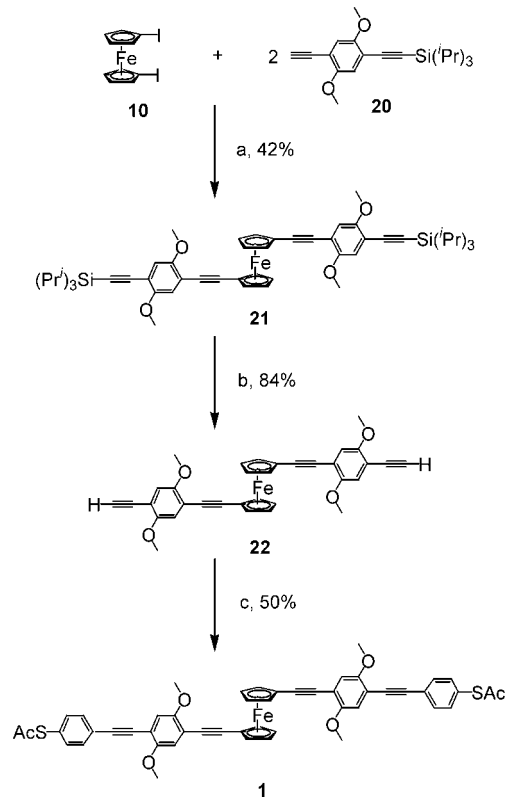

[a] $Pd(PPh_3)_2Cl_2$, $Cu(OAc)_2$, THF, Hunig's base, 90 °C, 24 h. (b) TBAF (2.2 equiv), CH_2Cl_2, RT, 15 min. (c) (i) **11**, $Pd(PPh_3)_2Cl_2$, CuI, THF, Hunig's base, 55 °C, 24 h.

(13) (a) Doisneau, G.; Balavoine, G.; Fillebeen-Khan, T. *J. Organomet. Chem.* **1992**, *425*, 113–117. (b) Ingham, S. L.; Khan, M. S.; Lewis, J.; Long, N. J.; Raithby, P. R. *J. Organomet. Chem.* **1994**, *470*, 153–159. (c) Lavastre, O.; Even, M.; Dixneuf, P. H.; Pacreau, A.; Vairon, J.-P. *Organometallics* **1996**, *15*, 1530–1531. (d) Long, N. J.; Martin, A. J.; Vilar, R.; White, A. J. P.; Williams, D. J.; Younus, M. *Organometallics* **1999**, *18*, 4261–4269. (e) Lindner, E.; Zong, R.; Eichele, K. *Phosphorus, Sulfur Silicon Relat. Elem.* **2001**, *168–169*, 543–546. (f) Gonzalez-Cabello, A.; Vazquez, P.; Torres, T. *J. Organomet. Chem.* **2001**, *637–639*, 751-–756. (g) Schottenberger, H.; Lukassser, J.; Reichel, E.; Muller, A. G.; Steiner, G.; Kopacka, H.; Wurst, K.; Ongania, K. H.; Kirchner, K. *J. Organomet. Chem.* **2001**, *637–639*, 558–576.

(14) (a) Inouye, M.; Hyodo, Y.; Nakazumi, H. *J. Org. Chem.* **1999**, *64*, 2704–2710. (b) Inouye, M.; Itoh, M. S.; Nakazumi, H. *J. Org. Chem.* **1999**, *64*, 9393–9398.

Scheme 8[a]

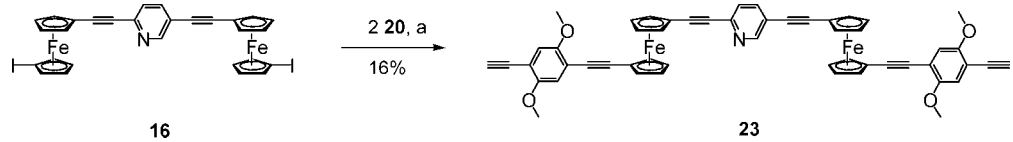

[a] (i) $Pd(PPh_3)_2Cl_2$, $Cu(OAc)_2$, THF, Hunig's base, 90° C, 24 h. (ii) TBAF (2.2 equiv), CH_2Cl_2, rt, 15 min.

Scheme 9[a]

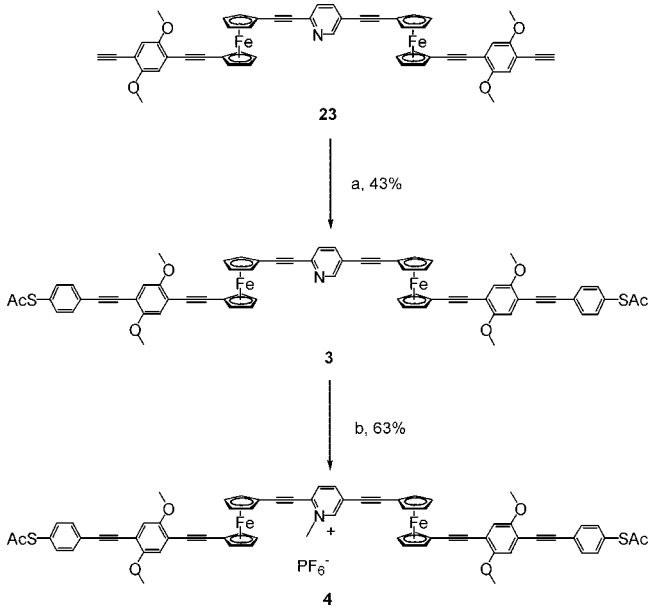

[a] (a) **11**, $Pd(PPh_3)_2Cl_2$, CuI, THF, Hunig's base, 55° C, 24 h. (b) (i) MeI, CH_2Cl_2/CH_3CN, 50° C, 18 h. (ii) H_2O, NH_4PF_6.

according to Scheme 2.[15] Consideration of this latter fact thus ultimately led us to settle upon 1-ethynyl-1′-iodoferrocene (**9**)[16,17] as the basic ferrocene-containing building block. Compound **9** has been prepared in low yield through a three-step process starting from 1,1′-diiodoferrocene (**10**);[18] however, for obtaining large quantities of this desired material, the two-step route shown in Scheme 3 proved to be highly efficient. In this process, a substoichiometric amount of triisopropylsilylacetylene and dilute conditions were used in palladium-catalyzed Sonogashira coupling to first produce a crude product containing unreacted **10** and a mono-silylacetylene-coupled intermediate, which was not isolated, but rather, desilylated with tetrabutylammonium fluoride (TBAF) to produce a mixture of **9** and **10** that could be easily separated by column chromatography on silica gel. In this fashion, pure **9** was reproducibly obtained in a 60% yield based on recovered **10**.

In retrospect, the ease with which compound **9** could be prepared through mono-Sonogashira coupling of **10** with an acetylene, without any significant coproduction of the possible 1,1′-dialkyne biscoupled product, revealed early on a critical disadvantage associated with using **9** and this coupling chemistry for construction of the targeted ferrocene frameworks. More specifically, over time, a large number of coupling reactions served to empirically show that, after introduction of the first alkyne substituent starting with **10**, the reactivity of the remaining iodo group of the monocoupled product toward subsequent Sonogashira coupling is greatly reduced for most classes of alkynes, an observation apparently not reported upon previously in the literature. On the other hand, this reduced activity of the iodo group in **9** allows one to perform Sonogashira couplings of the acetylene moiety with a wide variety of aryl iodides without any significant self-condensation polymerization occurring. Thus, using *S*-acetyl-4-iodothiophenol (**11**),[19] ferrocene **12** could be prepared in high yield according to eq 1 of Scheme 4. Unfortunately, attempts to couple 2 equiv of **12** with 2,5-diethynylpyridine (**13**)[20] failed to directly produce the diferrocene **14** (see eq 2 in Scheme 4). Likewise, while coupling of 2 equiv of **9** with 2,5-diiodopyridine (**15**) smoothly provided the 2,5-diethynylpyridine-linked diferrocene **16** (eq 3 in Scheme 4), subsequent attempts to extend the molecular framework of this compound through additional alkyne couplings mostly came up empty handed, as exemplified by the best of these experiments in which only a trace amount of the diferrocene **17** could be identified after attempted coupling with 1,4-diethynylbenzene[21] using Buchwald's and Fu's[22] $(PhCN)_2PdCl_2/P(t\text{-}Bu)_3$ catalyst combination according to eq 4 of Scheme 4. Interestingly, this general lack of reactivity of the iodo group of 1-alkynyl,1′-iodo ferrocenes toward alkyne coupling did not appear to extend to silylacetylenes, as shown by the ability to convert diferrocene **18** (*vide infra*) into the alkyne-coupled product **19** in high yield as shown in Scheme 5. Unfortunately, all attempts to desilylate **19** for further framework extension led to a complex product mixture, potentially as a result of a similar tendency of the deprotected alkyne moiety to undergo nucleophilic attack as previously depicted for 1,1′-diethynylferrocene in Scheme 2.

Although all synthetic routes to the desired diferrocene adsorbates now looked doomed, a fortunate decision was made to address another potential problem associated with the final target molecules, namely, that of limited solubility. On the basis of literature precedence, it was anticipated that as the conjugated molecular frameworks became more extended, they should also become increasingly less soluble. To compensate for this lack of solubility, a common practice is to place solubilizing substituents, in the form of either linear alkyl or alkyl ether chains, on phenyl rings.[23] In the present case, methoxy groups were adopted for this purpose given the ease with which they

(15) Pudelski, J. K.; Callstrom, M. R. *Organometallics* **1994**, *13*, 3095–3109.
(16) Butler, I. R.; Boyes, A. L.; Kelly, G.; Quayle, S. C.; Herzig, T.; Szewczyk, J. *Inorg. Chem. Commun.* **1999**, *2*, 403–406.
(17) For syntheses of the bromo analogue of **9**, see ref 16. Rosenblum, M.; Brawn, N. M.; Ciappenelli, D.; Tancrede, J. *J. Organomet. Chem.* **1970**, *24*, 469–477.
(18) Butler, I. R.; Wilkes, S. B.; McDonald, S. J.; Hobson, L. J.; Taralp, A.; Wilde, C. P. *Polyhedron* **1993**, *12*, 129–131.
(19) Pearson, D. L.; Tour, J. M. *J. Org. Chem.* **1997**, *62*, 1376–1387.
(20) Bunten, K. A.; Kakkar, A. K. *Macromolecules* **1996**, *29*, 2885–2893.
(21) Bodwell, G. J.; Miller, D. O.; Vermeij, R. J. *Org. Lett.* **2001**, *3*, 2093–2096.
(22) Hundertmark, T.; Littke, A. F.; Buchwald, S. L.; Fu, G. C. *Org. Lett.* **2000**, *2*, 1729–1731.
(23) (a) Creager, S.; Yu, C. J.; Bamdad, C.; O'Connor, S.; MacLean, T.; Lam, E.; Chong, Y.; Olsen, G. T.; Luo, J. Y.; Gozin, M.; Kayyem, J. F. *J. Am. Chem. Soc.* **1999**, *121*, 1059–1064. (b) Sikes, H. D.; Smalley, J. F.; Dudek, S. P.; Cook, A. R.; Newton, M. D.; Chidsey, C. E. D.; Feldberg, S. W. *Science* **2001**, *291*, 1519–1523. (c) Yu, C. J.; Chong, Y.; Kayyem, J. F.; Gozin, M. *J. Org. Chem.* **1999**, *64*, 2070–2079.

Scheme 10[a]

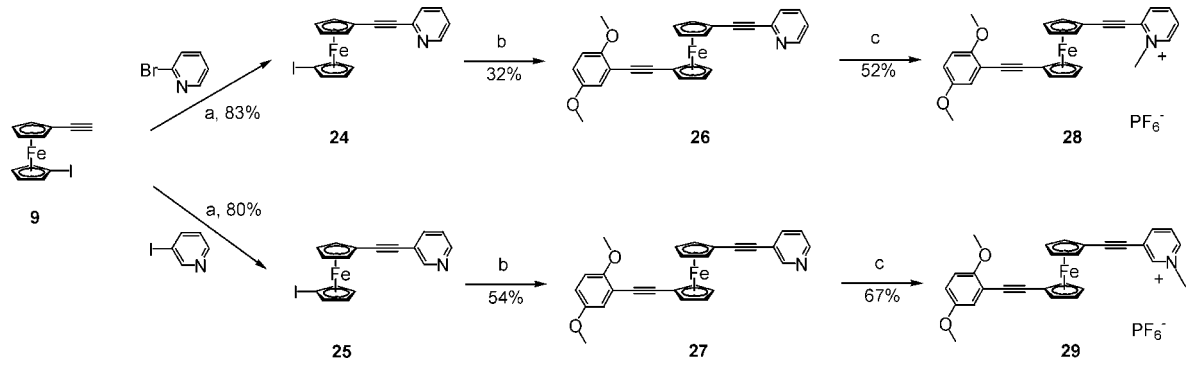

[a] (a) $Pd(PPh_3)_2Cl_2$, CuI, THF/Hunig's base (1:1), 50° C, 24 h. (b) (2,5-Dimethoxyphenyl)ethyne, $Pd(PPh_3)_2Cl_2$, $Cu(OAc)_2$, THF, Hunig's base, 60° C, 24 h. (c) (i) MeI, CH_2Cl_2, CH_3CN, 50° C, 18 h, (ii) H_2O, NH_4PF_6.

Scheme 11[a]

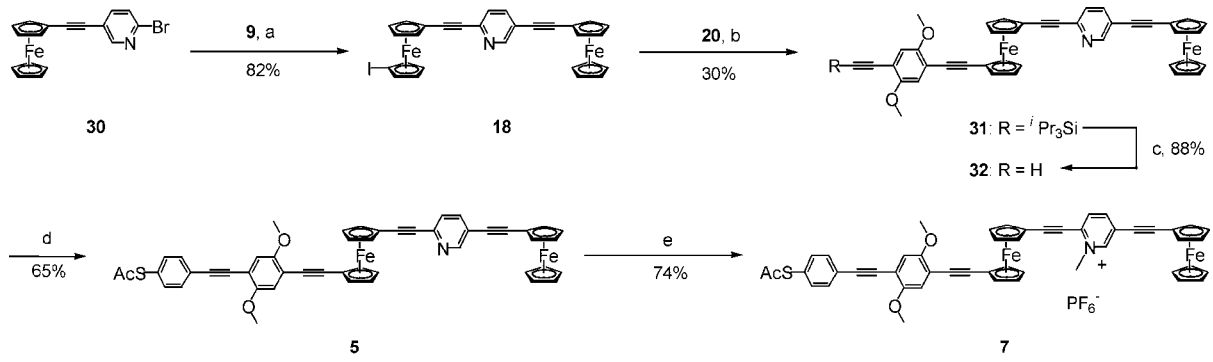

[a] (a) $Pd(PPh_3)_2Cl_2$, CuI, THF/Hunig's base (1:1), 55° C, 18 h. (b) $Pd(PPh_3)_2Cl_2$, $Cu(OAc)_2$, THF, Hunig's base, 55° C, 24 h. (c) TBAF (1.1 equiv), CH_2Cl_2, rt, 15 min. (d) **11**, $Pd(PPh_3)_2Cl_2$, CuI, THF, Hunig's base, 55° C, 24 h. (e) (i) MeI, CH_2Cl_2/CH_3CN, 50 °C, 18 h. (ii) H_2O, NH_4PF_6.

Scheme 12[a]

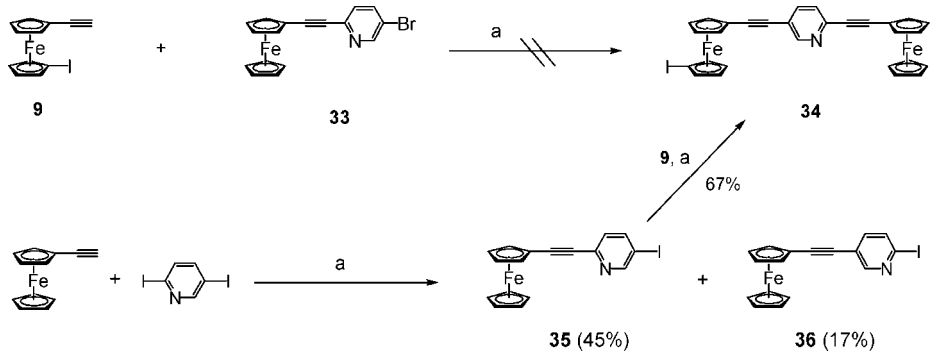

[a] (a) $Pd(PPh_3)_2Cl_2$, CuI, THF/Hunig's base (1:1), 55° C, 18 h.

could be incorporated into synthetic schemes and the minimum disturbance that they were expected to exert on packing within SAM structures. Thus, the bisalkyne derivative **20** in Scheme 6 was first prepared from 1-bromo-4-iodo-2,5-dimethoxybenzene[24] in a similar fashion to the method reported by Höger and Enkelmann[25] for similar compounds. Fortunately, with this building block in hand, it was quickly discovered that, like silylacetylenes, it was far more reactive in Sonogashira coupling with **9**, **10**, and 1-alkynyl,1′-iodo ferrocenes in general, so that 1,1′-bisalkyne ferrocenes could now be reliably prepared. For example, as Scheme 7 shows, coupling of 2 equiv of **20** with **10** now proceeded in modest yield to provide the symmetrically derivatized ferrocene **21**, which after clean desilylation provided the deprotected bisalkyne **22**. Compound **22** was then used in turn to prepare dithioacetate-protected **1** through coupling with 2 equiv of **11**.

The successful synthesis of the symmetric diferrocene framework of **1** encouraged us to return to the synthesis of the diferrocene thioacetates using the bisalkyne **20**. As shown in Scheme 8, coupling of **20** with the diferrocene core structure

(24) Orito, K.; Hatakeyama, T.; Takeo, M.; Suginome, H. *Synthesis* **1995**, *10*, 1273–1277.

(25) Hoger, S.; Enkelmann, V. *Angew. Chem., Int. Ed. Engl.* **1996**, *34*, 2713–2716.

Scheme 13[a]

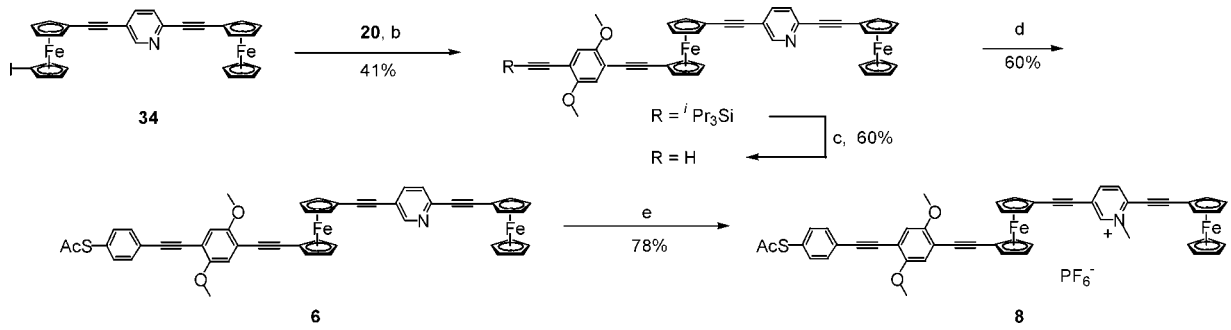

[a] (a) $Pd(PPh_3)_2Cl_2$, CuI, THF/Hunig's base (1:1), 55 °C, 18 h. (b) $Pd(PPh_3)_2Cl_2$, $Cu(OAc)_2$, THF, Hunig's base, 55 °C, 24 h. (c) TBAF (1.1 equiv), CH_2Cl_2, rt, 15 min. (d) **11**, $Pd(PPh_3)_2Cl_2$, CuI, THF, Hunig's base, 55 °C, 24 h. (e) (i) MeI, $CHCl_2/CH_3CN$, 50 °C, 18 h. (ii) H_2O, NH_4PF_6.

Scheme 14[a]

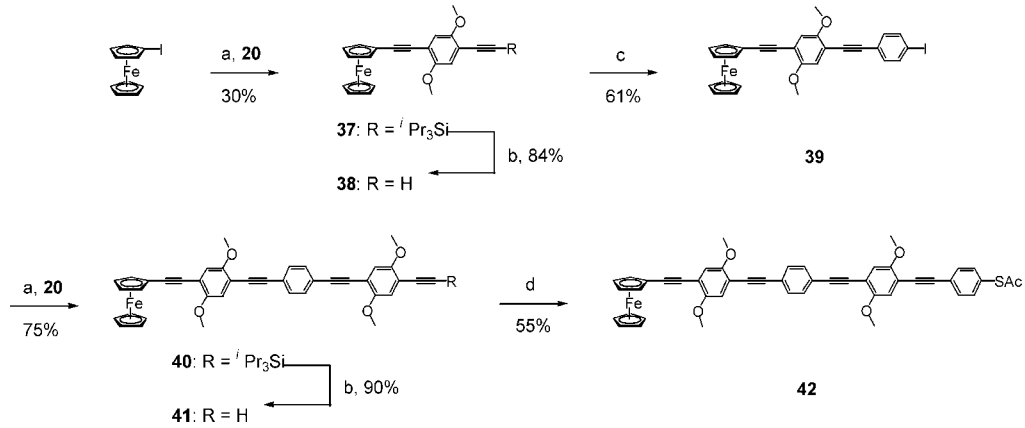

[a] (a) $Pd(PPh_3)_2Cl_2$, CuI, THF/Hunig's base (1:1), 55 °C, 18 h. (b) TBAF (1.1 equiv), CH_2Cl_2, rt, 15 min. (c) Diiodobenzene, $Pd(PPh_3)_2Cl_2$, CuI, THF/Hunig's base (1:1), 55 °C, 18 h. (d) **11**, $Pd(PPh_3)_2Cl_2$, CuI, THF/Hunig's base (1:1), 55 °C, 18 h.

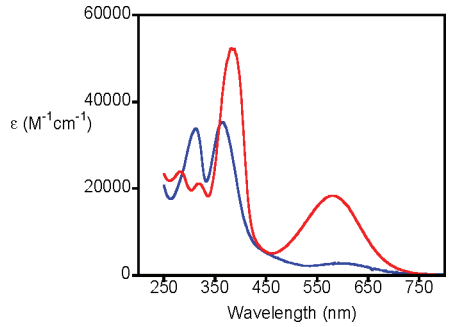

Figure 1. Comparison of electronic spectra for **4** (blue) and **44** (red) in CH_2Cl_2.

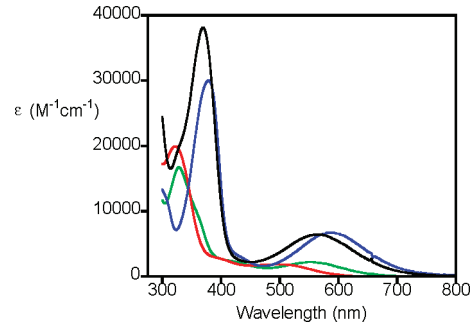

Figure 2. Comparison of electronic spectra for the 1-ethynylpyridine-1′-(dimethoxyphenyl)ethyne monoferrocenes, **28** (green) and **29** (red), and the 2,5-diethynylpyridyl-derivatized monoferrocenes, **45** (black) and **46** (blue), in CH_2Cl_2.

16now did indeed produce a reliable, although low yield, quantity of the desired extended bisalkyne **23** after standard desilylation. It is highly possible, however, that recently reported modifications and advances in catalysts for the Sonogashira coupling reaction may serve to considerably increase the yield of **23** in the future.[26] For now, the fact that **23** could be easily separated from a small amount of a regioisomeric mixture of monocoupled products through column chromatography allowed us to carry on with the synthesis of the final target molecules, **3** and **4** shown in Scheme 9. Thus, **23** was coupled with 2 equiv of **11** to provide **3** in reasonable yield, and **3** was then methylated to provide **4** with a similar degree of success.

Inclusion of the methoxy groups in the structures of **3** and **4** that were necessitated for synthetic reasons, but which were not

Chart 3

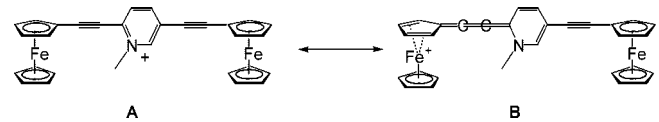

part of our previously published preliminary studies on 2,5-diethynylpyridine-linked diferrocenes,[6] caused us to consider what

(26) (a) See for instance: Thorand, S.; Krause, N *J. Org. Chem.* **1998**, *63*, 8551–8553. (b) Mio, M. J.; Kopel, L. C.; Braun, J. B.; Gadzikwa, T. L.; Hull, K. L.; Brisbois, R. G.; Marworth, C. J.; Grieco, P. A. *Org. Lett.* **2002**, *4*, 3199–3202. (c) Jones, T. V.; Blatchly, R. A.; Tew, G. N. *Org. Lett.* **2003**, *5*, 3297–3299.

Table 1. Cyclic Voltammetry (CV) and Differential Pulse Voltammetry (DPV) Analysis of 1,1′-Diethynyl-Derivatized Ferrocenes[a]

	CV		DPV	
compound	$E^1_{1/2}$	$E^2_{1/2}$	$E^1_{1/2}$[b,c]	$E^2_{1/2}$[b,c]
3	0.939[d]		0.944 (2)	
4	1.04	1.23	1.04 (1)	1.23 (1)
5	[e]		0.861 (1)	0.987 (1)
6	[e]		0.877 (1)	0.975 (1)
7	0.958	1.25	0.950 (1)	1.26 (1)
8	1.10[d]		1.11 (2)	
26	0.943		0.941 (1)	
27	0.938		0.937 (1)	
28	1.20		1.21 (1)	
29	1.08		1.09 (1)	
43	0.840		0.818 (2)	
44	0.955	1.12	0.929 (1)	1.90 (1)
45	1.01		1.01 (1)	
46	1.13		1.14 (1)	

[a] Recorded at 298 K using 1 mM of the compound in 0.1 M [*n*-Bu_4N][$B(C_6F_5)_4$] in CH_2Cl_2 using a glassy carbon working electrode, a Pt wire counter electrode, and a Ag/Ag+ reference electrode. Values are reported relative to the redox couple of a known amount of decamethylferrocene (Cp^*_2Fe) added as an internal standard. [b] Calculated from $E_{pk} = E_{1/2} -$ pulse amplitude/2. [c] Values in parentheses are the integrated number of electrons based on the known amount of Cp^*_2Fe added as an internal standard. [d] Two unresolved (overlapping) one-electron processes. [e] $E_{1/2}$ values not determined since peaks were not fully resolved by CV.

effect a donor–acceptor interaction within the conjugated framework (i.e., between 2,5-dimethoxyphenyl and pyridinium groups) might have on the electronic structure, and thus the electron transport properties, of an intervening ferrocene moiety. To probe this question, the regioselective syntheses of the model complexes shown in Scheme 10 were developed. To begin, compound **9** was first coupled with commercially available 2-bromopyridine to provide the pyridyl ferrocene **24** in high yield. Under similar conditions, however, 3-bromopyridine failed to couple to provide the desired regioisomer. This compound, **25**, was obtained by coupling **9** with 3-iodopyridine[27] instead. Next, both **24** and **25** were coupled with (2,5-dimethoxyphenyl)ethyne[28] to provide the regioisomeric compounds **26** and **27**, respectively. Finally, compounds **26** and **27** were methylated to produce the desired model complexes **28** and **29** as shown in Scheme 10.

The regiospecific synthesis of the desired monothiol diferrocene adsorbates **5** and **6** for inclusion into SAMs proved to be straightforward in the case of isomer **5**, as shown in Scheme 11. Thus, coupling of the previously reported ferrocene pyridyl bromide **30**[6] with **9** first provided **18**, which was then coupled with **20** to generate product **31**, which was subsequently desilylated to yield the deprotected alkyne **32**. Coupling of **32** with **11** finally provided the monothioacetate **5** in 65% yield, and this compound was then methylated to produce the pyridinium complex **7**.

In sharp contrast to the straightforward route to **5**, synthesis of the regioisomer **6** proved to be slightly more challenging in that an analogous coupling of **9** with the previously reported ferrocene pyridyl bromide **33**[6] failed to provide compound **34** according to Scheme 12. A successful route to **34** was eventually found, however, by using the iodo analogue **35**, which was inelegantly, but effectively, prepared through coupling of ethynylferrocene[29] with 2,5-diiodopyridine[30] to produce a mixture of **35** and its regioisomer **36**. Fortunately, **35** could be isolated in pure form through column chromatography in a 45% yield, and single-crystal X-ray analysis was used to confirm that its molecular structure was indeed the required regioisomer.

With **34** in hand, the synthesis of compound **6** was rapidly finished according to the route shown in Scheme 13. More precisely, coupling of **34** with **20**, followed by desilylation and coupling with **11**, provided **6** in a 15% overall yield from **34**. Methylation then provided the pyridinium complex **8**.

Finally, in order to compare the rate of electron transfer through an intervening ferrocene moiety versus a phenyl group within molecular frameworks of comparable length,[12] the thioacetate-protected ferrocene-terminated phenylethynyl oligomer **42** was prepared in straightforward fashion according to Scheme 14 through the intermediates **37**−**41**.

(b) Electronic Spectra. As mentioned previously, methoxy groups were added to the targeted diferrocence frameworks in order to enhance solubility characteristics; however, it was understood from the start that these formal electron-donating groups might be noninnocent bystanders with regard to contributions made to the overall electronic structure of the system. In particular, for the pyridinium cations, **4**, **7**, and **8**, it might be expected that significant donor (2,5-dimethoxyphenyl)/acceptor (pyridinium) interactions could influence rates of electron transport across the intervening ferrocene moiety. Thus, to begin to understand in what manner the methoxy groups might be perturbing electronic structure, electronic (UV/vis) spectra of these compounds were recorded and compared with those taken of the model compounds, **28**, **29**, and the previously reported species, **43**–**46**.[6] To begin, Figure 1 compares the electronic spectrum of **44** with that of **4** as recorded in CH_2Cl_2. As can be seen, the relatively strong metal-to-ligand charge transfer (MLCT) absorption observed for **44** at 582 nm (ϵ_{max} 18 380) is greatly attenuated in **4**, which exhibits a corresponding MLCT at 600 nm (ϵ_{max} 2 760). No new charge transfer band is observed for **4** that might be attributable to a direct donor–acceptor interaction between the 2,5-dimethoxyphenyl and pyridinium groups. These data are taken as evidence that the 2,5-dimethoxyphenylethynyl "arms" on each ferrocene in **4** actually serve as *electron-withdrawing* substituents that decrease the donor strength of the metal for MLCT. A comparison of the electronic spectra for **28**, **29**, **45**, and **46** shown in Figure 2 reveals a similar attenuation of the MLCT band between corresponding structural pairs, and now one can also determine what role the position of the nitrogen atom within the pyridinium moiety plays in determining the strength of the MLCT. As can be seen, when the pyridinium nitrogen is facing toward the ferrocene as in **28**, there is a significant bathochromic shift of the MLCT band relative to the corresponding regioisomer **29** in which the pyridinium nitrogen is facing away from the ferrocene [cf. for **28**, λ_{max} 554 nm (ϵ_{max} 2 200) vs for **29**, λ_{max} 496 nm (ϵ_{max} 1 890)]. This trend, which is also observed for the **45/46** pair of compounds, reinforces our original proposal[6] that, on the basis of the resonance scheme presented in Chart 3, a lower energy MLCT will be observed for the ferrocene that is in an *ortho* relationship to the pyridinium cation acceptor due to the "strong electronic communication" that exists by way of the direct delocalization pathway shown (see structure **B** in Chart 3). In corollary fashion, a ferrocene positioned in a *meta* relationship to the pyridinium cation acceptor is in weaker, more indirect, electronic communication.

(27) Trecourt, F.; Breton, G.; Bonnet, V.; Mongin, F.; Marsais, F.; Queguiner, G. *Tetrahedron* **2000**, *56*, 1349–1360.
(28) Buckle, D. R.; Rockell, C. J. M. *J. Chem. Soc., Perkin Trans. 1* **1985**, *11*, 2443–2446.
(29) Polin, J.; Schottenberger, H. *Org. Synth.* **1996**, *73*, 262–269.
(30) Hama, Y.; Nobuhara, Y.; Aso, Y.; Otsubo, T.; Ogura, F. *Bull. Chem. Soc. Jpn.* **1988**, *61*, 1683–1686.

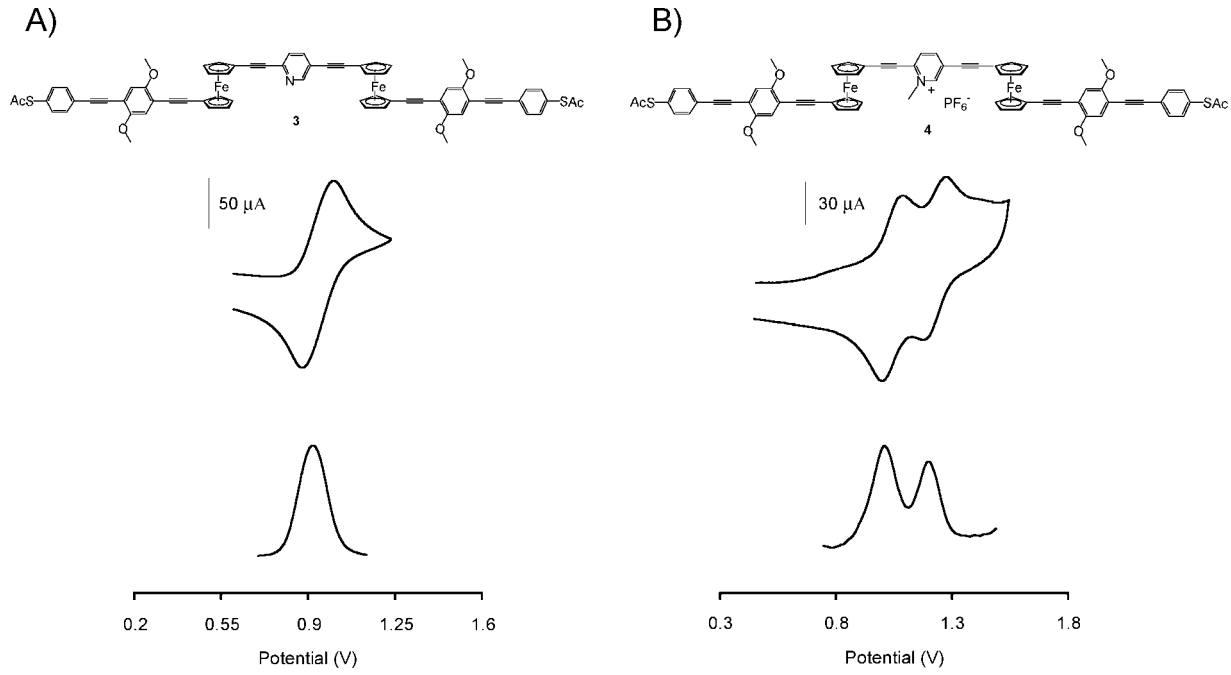

Figure 3. CV, scan rate 0.1 Vs^{-1} (top) and DPV (bottom) for (A) **3** and (B) **4** in 0.1 M [*n*-Bu_4N][$B(C_6F_5)_4$] in CH_2Cl_2 using a glassy carbon working electrode. Potentials are referenced to the internal standard, Cp^*_2Fe.

(c) Solution Electrochemistry. A comprehensive investigation of the electrochemical properties of the newly synthesized compounds, **3**–**8** [X = $COCH_3$ (Ac)], was conducted in order to study the redox properties of the ferrocene units within these extended conjugated frameworks. For comparison purposes, the electrochemical properties of the model complexes **43**–**46** were once again used. Table 1 presents data obtained from dc cyclic voltammetry (CV) and differential pulse voltammetry (DPV) analysis of the listed compounds, and Figure 3 presents in graphical format the CV and DPV data obtained for compounds **3** and **4**. To begin, it should be pointed out that since many of the electrochemical studies involved *in situ* formation of di- and tricationic species upon full oxidation, the non-nucleophilic supporting electrolyte, [(*n*-$Bu)_4N$][$B(C_6F_5)_4$] in CH_2Cl_2, that was introduced by Geiger and co-workers,[31] was employed. Under these conditions, all redox couples were observed to be either reversible or quasi-reversible processes at a glassy carbon working electrode as assessed by the width of peaks at half-height.[32] As shown in Figure 3A, compound **3** displays a single unresolved redox couple for the two ferrocenes, which means that the redox potentials of these two moieties must be within a few tens of millivolts of one another.[33] Viewed another way, as previously determined for **43**,[6] the unsymmetric 2,5-diethynylpyridyl unit of **3** is sufficiently long enough so that the two ferrocene groups of **3** do not experience any significant electostatic repulsion between one another upon oxidation,[34] nor does the unsymmetric nature of this bridging group preferentially perturb the electronic structure of one ferrocene significantly over the other. Upon placing a positive charge on the pyridyl nitrogen, however, the asymmetry of the bridging pyridinium cation in **4** has a profound differential influence on the two ferrocene groups, resulting in two one-electron redox couples now being observed with a $\Delta E_{1/2}$ value of 190 mV (see Figure 3B). Once again, the resonance structures of Chart 3 account for the stronger perturbation imposed on a ferrocene moiety that is positioned in an *ortho* relationship to the pyridinium cation vis-à-vis a ferrocene that is in a *meta* position. In comparing the redox potentials of **3** and **4** with those of **43** and **44**, it is interesting, and important, to note that the conjugated 2,5-dimethoxyphenylethynyl "arms" in the former pair once again appear to act as electron-withdrawing groups that serve to shift their redox potentials to higher values relative to those of the latter pair (see Table 1). This apparent electron-withdrawing effect of a dimethoxy-substituted phenylethynyl group tells an even more interesting tale when analyzing the electrochemistry of the monothioacetate compounds, **5** and **6**, and their respective pyridinium derivatives, **7** and **8**.

Figure 4 presents the CV and DPV data for compounds **5**−**8**. Not unexpectedly, given the unsymmetric nature of the compound, the CV and DPV for **5** revealed two resolved one-electron redox couples for the two ferrocene groups ($\Delta E_{1/2}$ = 126 mV) (see Figure 4A). In going to the pyridinium structure, this separation of redox couples increases even further to a remarkable $\Delta E_{1/2}$ value of 310 mV for compound **7** as shown in Figure 4B. In contrast, as Figure 4C and 4D present, in the regioisomeric structures, a much smaller $\Delta E_{1/2}$ value is observed in each case: 98 mV for **6** and only ∼50 mV for **8**. While initially somewhat surprising, the electrochemical behavior of this latter pair of compounds is readily explained after considering the redox properties of the regioisomeric model monoferrocene compounds **28** and **29**, along with those of **45** and **46**. Thus, once again due to the contributing resonance form **B** of Chart III, it was established that a greater shift in the anodic direction of the half-wave potential of a ferrocene resulted when the electron-withdrawing pyridinium cation was in direct electronic communication with the ferrocene (i.e., with the nitrogen atom "facing toward" the iron center) as opposed to a weaker, more indirect communication (i.e., with the nitrogen atom "facing away from" the iron center) (see Table 1). Additionally, as presented in Table 1, the CV and DPV analyses for the two isomeric pyridinium cations, **28** and **29**, showed that an electron-withdrawing 2,5-dimethoxyphenylethynyl

(31) LeSuer, R. J.; Geiger, W. E. *Angew. Chem., Int. Ed.* **2000**, *39*, 248–250.

(32) Bard, A. J.; Faulkner, L. R. *Electrochemical Methods*; John Wiley & Sons, Inc.: New York, 2001.

(33) Barriére, F.; Geiger, W. E. *J. Am. Chem. Soc.* **2006**, *128*, 3980–3989, references cited therein.

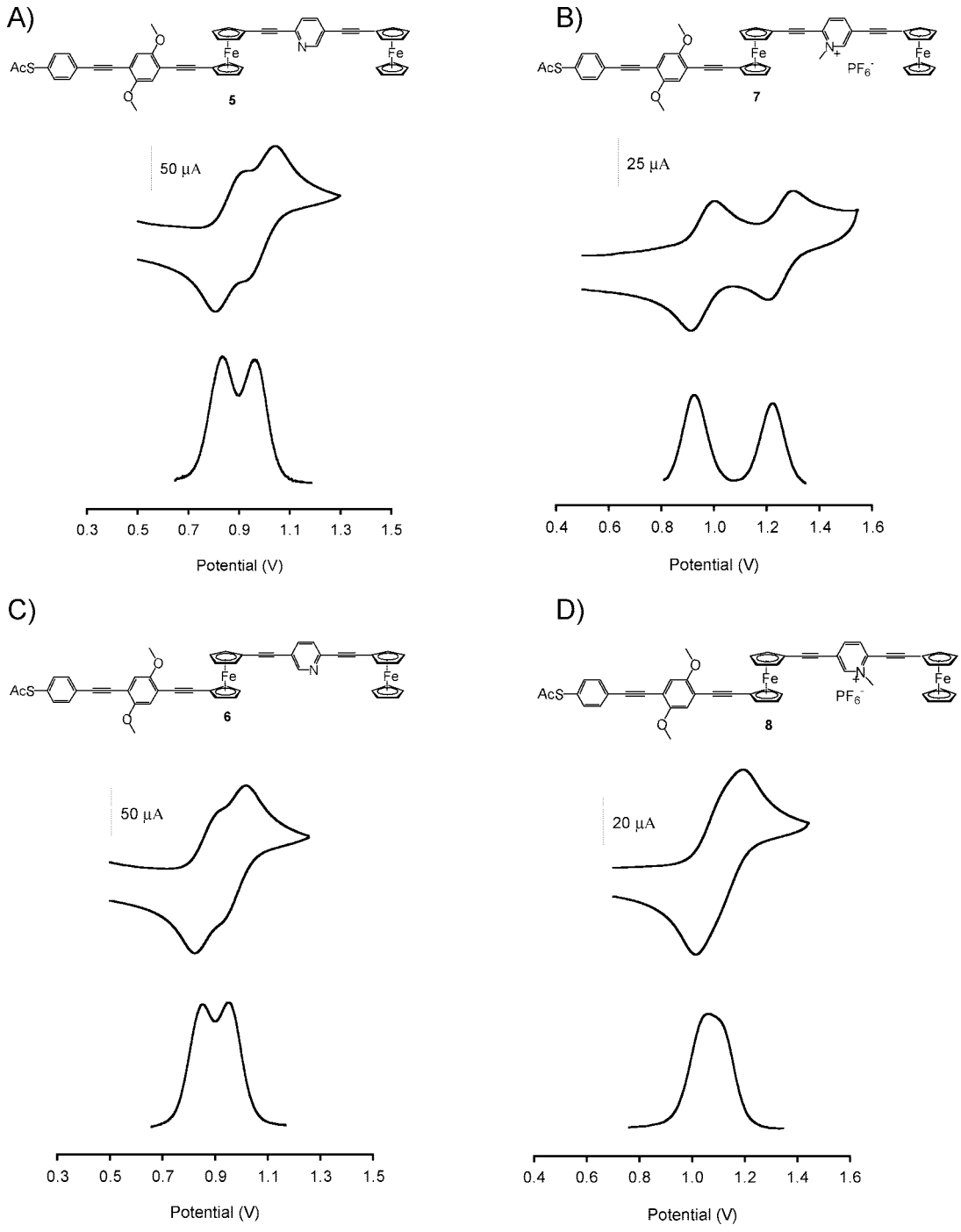

Figure 4. CV, scan rate 0.1 V s^{-1} (top) and DPV (bottom) for (A) **5**, (B) **7**, (C) **6**, and (D) **8** in 0.1 M [*n*-Bu_4N][$B(C_6F_5)_4$] in CH_2Cl_2 using a glassy carbon working electrode. Potentials are referenced to the internal standard, Cp^*_2Fe.

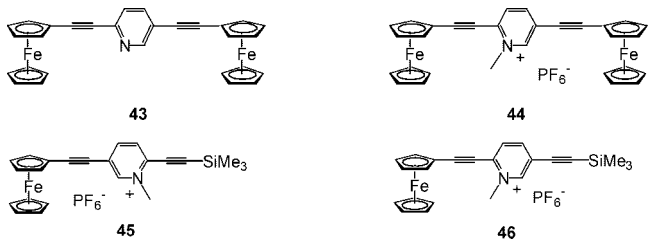

substituent on the cyclopentadienyl rings of the ferrocene resulted in the half-wave potential of ferrocene shifting to higher potential (anodic direction) relative to the half-wave potentials for the corresponding monoferrocene isomers **45** and **46**. Taken altogether, these data allow for the structure/electrochemical analyses of the diferrocene monothioacetates presented in Figure 5A, in which a close correlation between the $E_{1/2}$ values of **7** and **8** and those for the pairs of monoferrocene model compounds, **28/45** and **29/46**, respectively, is observed. In particular, the DPV analyses for compound **8** and the corresponding monoferrocene compounds **29** and **46** shown in Figure 5B clearly predict the presence of two one-electron redox couples with a $\Delta E_{1/2}$ value of approximately 50 mV in the diferrocene structure. As a final comment, it should also be noted that the greater separation in $E_{1/2}$ values observed for the regioisomeric compound **7** is the result of the redox potential of the internal ferrocene group being strongly influenced by both strong electronic communication with the pyridinium cation and the electron-withdrawing nature of the 2,5-dimethoxyphenylethynyl substituent.

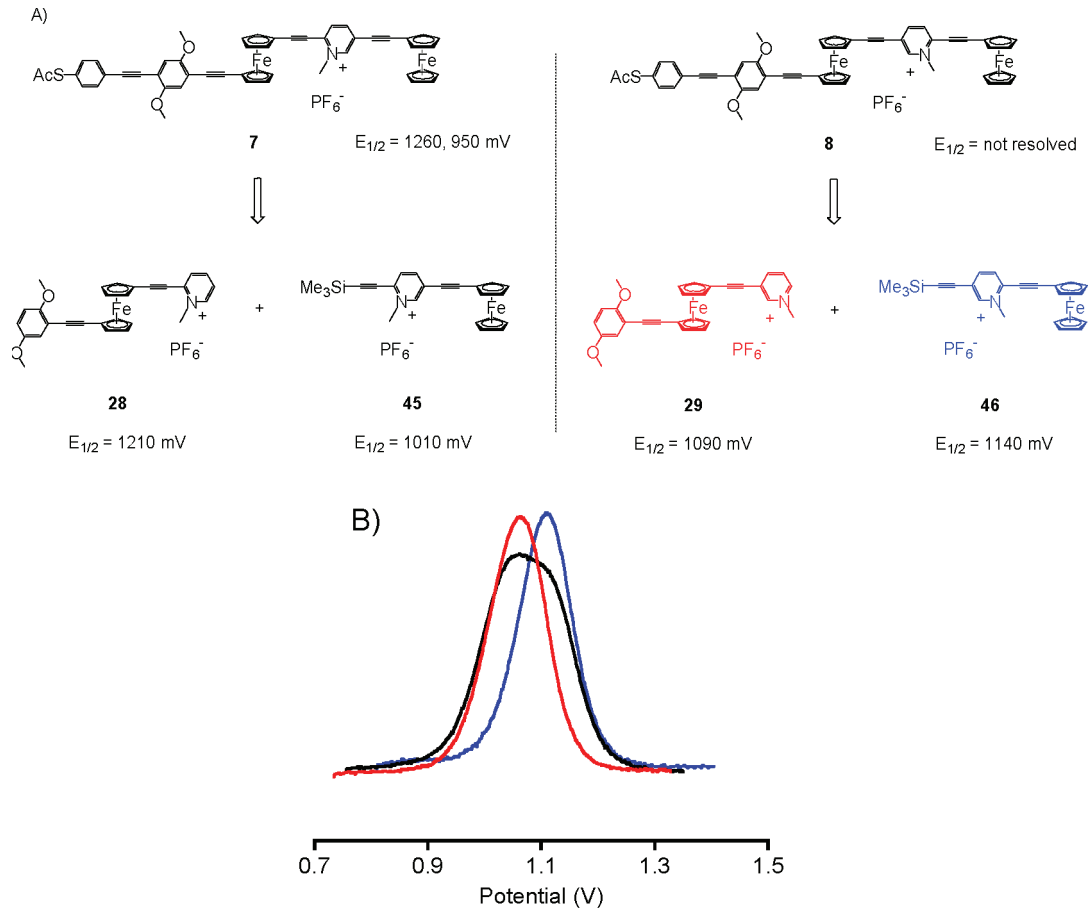

Figure 5. (A) Structural/electrochemical comparison of compounds **7** and **8** and their corresponding monoferrocene models. (B) Comparison of DPV data for **8** (black) and the two monoferrocene model compounds **29** (red) and **46** (blue), which predicts the two unresolved one-electron redox couples in the diferrocene compound **8**.

Conclusion

The present report serves several purposes in the quest for ferrocene-based molecular components that might be suitable for incorporation into future nanoscale electronic devices. First, we have documented regiospecific synthetic routes that should now make a variety of unsymmetric, phenylethynyl-conjugated mono- and diferrocene molecular frameworks with end-to-end distances of up to ~4 nm that are suitably derivatized with monothiol and α,ω-dithiol functionalities for their inclusion into a variety of LML heterojunction test structures. Second, we have been able to document the "noninnocent bystander" status of the 2,5-dimethoxyphenylethynyl moiety that can be globally treated as an electron-withdrawing substituent that serves to shift the Fe(II)/Fe(III) redox couple to higher potentials. This detailed knowledge of solution electrochemical behavior of compounds **3**–**8** should benefit efforts directed toward the fabrication and characterization of SAMs and LML heterojunctions in which these diferrocene frameworks are incorporated.[12]

Acknowledgment. This work was funded by the Basic Energy Sciences division of the Department of Energy (DEF-G0201ER15258) and in part by the NSF-NIRT (DMR-0102950) and NSF-MRSEC (DMR-0080008) programs, for which we are thankful.

Supporting Information Available: Full experimental details, including synthesis and analytical characterization of all new compounds and solution electrochemical characterization. This material is available free of charge via the Internet at http://pubs.acs.org.

OM700807X

(34) (a) Flanagan, J. B.; Margel, S.; Bard, A. J.; Anson, F. C. *J. Am. Chem. Soc.* **1978**, *100*, 4248–4253. (b) Daum, P.; Murray, R. W. *J. Phys. Chem.* **1981**, *85*, 389–396. (c) Rosenblum, M.; Nugent, H. M.; Jang, K. S.; Labes, M. M.; Cahalane, W.; Klemarczyk, R.; Reiff, W. M. *Macromolecules* **1995**, *28*, 6330–6342. (d) Watanabe, M.; Nagasaka, H.; Ogata, N. *J. Phys. Chem.* **1995**, *99*, 12294–12300. (e) Lee, W. Y.; Hostetler, M. J.; Murray, R. W.; Majda, M. *Isr. J. Chem.* **1997**, *37*, 213–223. (f) Xu, G. L.; Crutchley, R. J.; DeRosa, M. C.; Pan, Q.-J.; Zhang, H. X.; Wang, X.; Ren, T. *J. Am. Chem. Soc.* **2005**, *127*, 13354–13363. (g) Xu, G. L.; Xi, B.; Updegraff, J. B.; Protasiewicz, J. D.; Ren, T. *Organometallics* **2006**, *25*, 5213–5215. (h) Sun, H.; Steeb, J.; Kaifer, A. E. *J. Am. Chem. Soc.* **2006**, *128*, 2820–2821.